

Statistics of finite-time Lyapunov exponents in the Ulam map

Celia Anteneodo

*Centro Brasileiro de Pesquisas Físicas, R. Dr. Xavier Sigaud 150,
22290-180, Rio de Janeiro, Brazil*

(December 16, 2018)

The statistical properties of finite-time Lyapunov exponents at the Ulam point of the logistic map are investigated. The exact analytical expression for the autocorrelation function of one-step Lyapunov exponents is obtained, allowing the calculation of the variance of exponents computed over time intervals of length n . The variance is shown to anomalously decay as $1/n^2$. The probability density of finite-time exponents noticeably deviates from the Gaussian shape, decaying with exponential tails and presenting 2^{n-1} spikes that accumulate close to the mean value and narrow with increasing n . The asymptotic expression for this probability distribution function is derived. It provides an adequate smooth approximation to describe numerical histograms built for not too small n , where the finiteness of bin size trims the sharp peaks.

PACS numbers: 05.45.-a, 02.50.-r

INTRODUCTION

In a dynamical system, Lyapunov exponents (LE) quantify the average exponential rate of expansion or contraction of infinitesimal volume elements in each direction of phase-space. Negative exponents imply convergence of initially nearby trajectories, while positive ones mean exponential divergence of neighboring orbits. Whereas the former case is associated with regular motion, the latter denotes chaos.

Following Oseledec's theorem [1,2], the average rate of growth converges to a time asymptotic limit, λ_∞ , independently of the particular trajectory chosen, for almost all initial conditions. A useful generalization of the asymptotic LE is the finite-time or local LE, λ_n , calculated over a time interval of length n along a given trajectory [3]. In contrast to asymptotic ones, exponents defined for finite time depend on the initial conditions. The analysis of finite-time LE is particularly important as they are the quantities actually measured in computational studies, unavoidably performed for finite time. Local LE have proved to be useful in the characterization of a variety of phenomena ranging from two-dimensional turbulence [4] to the so-called Loschmidt echo [5]. These local exponents are fluctuating quantities that may even change sign depending on the degree of heterogeneity of the relevant subset of phase space. Their fluctuations give rise to a nontrivial probability density $P(\lambda_n)$ that asymptotically collapses to a Dirac delta function centered at λ_∞ . The deviations from this limit and the convergence to it contain rich information on the underlying dynamics [3,6].

A relevant question on the dynamics of chaotic systems is the existence or not of true trajectories lying close to the numerically generated ones. It is known that local LE fluctuating around zero cause the nonexistence of such shadowing trajectories [7]. Particularly, in the synchronization transition of lattices of coupled chaotic 1D maps [8], unshadowability of chaotic orbits is due to un-

stable dimension variability, characterized by the second largest LE fluctuating about zero [9]. The connection between the probability distribution function (PDF) of local LE in the synchronized states and the PDF of local exponents in the uncoupled map [10] motivates the study of the statistical properties of finite-time LE in chaotic maps. Within this context, the numerical nature of the difficulties involved makes analytical results specially relevant.

This work focuses on the statistical properties of local LE for the logistic map at a parameter value yielding fully developed chaos, namely, at the Ulam point, where $x \mapsto 4x(1-x)$. This particular mapping allows exact calculations that are expected to be useful for more general systems belonging to the same class of chaotic behavior. Firstly we will calculate the variance of local LE since this important quantity can be evaluated exactly. In order to do so, one will need to evaluate the autocorrelation function of one-step LE. Furthermore, we will investigate thoroughly the PDF of local LE. Taking as a starting point the work by Prasad and Ramaswamy [11], we will extend it by deriving an user-friendly expression for the PDF of finite-time LE, a very good approximation for not too small n .

LOCAL LYAPUNOV EXPONENTS

For a 1D map $x \mapsto f(x)$ with differentiable f , finite-time LE $\lambda(n)$, computed over the interval of length n , are given by [6]

$$\lambda_n = \frac{1}{n} \sum_{j=0}^{n-1} \ln |f'(x_j)|, \quad (1)$$

where $x_j = f^j(x_0)$ is the j^{th} iterate of the initial condition x_0 . We will compute local LE after a transient has elapsed, so that averages over different realizations

can be calculated with the weight given by the invariant density $p(x)$ of the chaotic attractor.

Random initial conditions yield fluctuations in the values of λ_n around $\langle \lambda_n \rangle = \lambda_\infty$, with variance $\sigma^2(n) = \langle \lambda_n^2 \rangle - \lambda_\infty^2$, that by means of (1) can be expressed as

$$\sigma^2(n) = \frac{1}{n^2} \sum_{j=0}^{n-1} \sum_{k=0}^{n-1} C_{j,k}, \quad (2)$$

where

$$C_{j,k} = \langle \ln |f'(x_j)| \ln |f'(x_k)| \rangle - \langle \ln |f'(x_j)| \rangle \langle \ln |f'(x_k)| \rangle \quad (3)$$

is the two-time autocorrelation function of one-step (unitary time) LE [12].

Separating diagonal from off-diagonal terms, one gets

$$\sigma^2(n) = \frac{1}{n^2} \sum_{k=0}^{n-1} C_{k,k} + \frac{2}{n^2} \sum_{j=0}^{n-1} \sum_{k>j}^{n-1} C_{j,k}. \quad (4)$$

After a transient, when stationarity has been attained, temporal translational invariance holds. In this case, correlations will depend on the two times only through their difference, so that

$$\sum_{j=0}^{n-1} \sum_{k>j}^{n-1} C_{j,k} = \sum_{m=1}^{n-1} [n-m] C(m), \quad (5)$$

where $C(m) \equiv C_{0,m}$, and additionally $C(0) \equiv C_{0,0} = C_{m,m}, \forall m$. Hence,

$$\sigma^2(n) = \frac{1}{n} C(0) + \frac{2}{n^2} \sum_{m=1}^{n-1} [n-m] C(m). \quad (6)$$

Higher moments would require the calculation of correlation functions involving several times.

In order to evaluate the variance explicitly, one must compute the autocorrelation function C characteristic of the particular mapping f considered. In what follows, we will perform the explicit calculations for the logistic map $f(x) = \mu x(1-x)$ at $\mu = 4$, with $x \in [0, 1]$ (usually called Ulam map).

TIME CORRELATIONS IN THE ULAM MAP

For this logistic map the dynamics is exactly solvable (see, for instance, [3,13]). In fact, using the change of variables $z = 2 \arcsin(\sqrt{x})/\pi$, it is easy to find that the j^{th} iterate is $x_j = \sin^2(2^{j-1} \pi z_0)$. The time evolution for the new variable is given by the *tent* map $z \mapsto 1 - 2|z - 1/2|$, with $z \in [0, 1]$ [3,13]. The invariant density, $p(x) = [\pi \sqrt{x(1-x)}]^{-1}$, becomes uniform for $z \in [0, 1]$. In the z -representation, the required correlations can be straightforwardly obtained by following

the procedure of Nagashima and Haken [14] to calculate the time autocorrelation function $C_H(m)$,

$$C_H(m) = \langle H(g^m(z)) H^*(z) \rangle - \langle H(g^m(z)) \rangle \langle H^*(z) \rangle, \quad (7)$$

of an arbitrary function $H(z)$ where z evolves through the mapping $g(z)$ and $*$ denotes complex conjugate. The basic idea is to consider the Fourier expansion

$$H(g^m(z)) = \sum_{k=-\infty}^{\infty} a_k^m e^{2\pi i k z}, \quad m = 0, 1, 2, \dots, \quad (8)$$

where

$$a_k^m = \int_0^1 dz H(g^m(z)) e^{-2\pi i k z}. \quad (9)$$

In our case $H(z) = \ln |4 \cos(\pi z)|$, then it is indifferent if we evolve z either with the tent map or with the Bernoulli shift $g(z) = 2z \pmod{1}$ that will generate the same sequence $H(g^m(z))$. We will consider the latter case in order to use the results of [14]. Recursively, they arrive at

$$a_k^m = \begin{cases} a_j^0 & \text{if } k = 2^m j; j \in \mathcal{Z} \\ 0 & \text{otherwise.} \end{cases} \quad (10)$$

Then, using (7), (8), (10) and additionally considering that $\langle H(z) \rangle = \langle H(g^m(z)) \rangle = a_0^0, \forall m$, the correlation results

$$C_H(m) = \sum_{k \neq 0} a_k^0 a_{2^m k}^{0*}. \quad (11)$$

Now, for our particular case we have

$$a_l^0 = \frac{2}{\pi} \int_0^{\pi/2} dy \ln(\cos y) \cos(2ly), \quad (12)$$

that gives

$$a_l^0 = \begin{cases} -\ln 2, & \text{if } l = 0 \\ -\frac{(-1)^l}{2^l}, & \text{otherwise.} \end{cases} \quad (13)$$

Substituting these coefficients into (11), we obtain the following exact expression for the stationary autocorrelation of one-step LE:

$$C(m) = \begin{cases} \frac{\pi^2}{12}, & \text{if } m = 0 \\ -\frac{\pi^2}{24} \frac{1}{2^m}, & \text{otherwise.} \end{cases} \quad (14)$$

The autocorrelation function decays exponentially fast with time, with a characteristic time that is the inverse of $\lambda_\infty = \ln 2$. Although the sequence $\{x_j\}$ generated by the Ulam map is δ -correlated (more precisely,

$C_x(m) = \langle x_j x_{j+m} \rangle - \langle x_j \rangle \langle x_{j+m} \rangle = \frac{1}{8} \delta_{0m}$ [15]), correlations of higher powers of x_j do not decay to zero immediately [16], leading to the exponential decay of the autocorrelation of one-step LE.

Once the autocorrelation (14) is known, from Eq. (6), we obtain

$$\sigma^2(n) = \frac{\pi^2}{6n^2} \left(1 - \frac{1}{2^n}\right). \quad (15)$$

It is noteworthy that the variance decays with time as $1/n^2$. If the terms of the sum in Eq. (1) were independent, then the decay should be as $1/n$. However, those terms are highly dependent: The sum can be expressed as a function of the single variable x_0 through the map successive iterates $f^j(x_0)$. This is a nice example illustrating that linear correlation and dependence are quite different statistical concepts. Naturally, although the correlations decay exponentially fast, the central limit theorem will not hold in this case.

PDF OF LOCAL EXPONENTS

Given a PDF $\rho_X(x)$, the standard formula for the PDF $\rho_Y(y)$, such that $y = \phi(x)$, is

$$\rho_Y(y) = \int \rho_X(x) \delta(y - \phi(x)). \quad (16)$$

Prasad and Ramaswamy have already presented [11] the exact although hermetic expression for the PDF $P(\lambda_n)$ of local LE on the Ulam map, that comes immediately from the knowledge of the invariant measure $p(x)$, using (16). In fact, from Eq.(1), one can write $\lambda_n = \ln[G_n(x)]/n$, with $G_n(x) = 4^n \prod_{j \geq 0}^{n-1} |1 - 2f^j(x)|$. Then, one has

$$P(\lambda_n) = \int_0^1 dx p(x) \delta(\lambda_n - \ln[G_n(x)]/n), \quad (17)$$

giving

$$P(\lambda_n) = n \exp(n\lambda_n) \sum_{\text{roots}} \frac{p(x)}{|G'_n(x)|}, \quad (18)$$

where the summation runs over all real roots of the $(2^n - 1)$ -order polynomial $G_n(x) - \exp(n\lambda_n)$. Because $G_n(x)$ is odd order, there is always at least one real root. For λ_n below the mean value, all roots are real. As λ_n increases above the mean value, the roots leave the real axis by pairs. At each point where this occurs, $G'_n(x) = 0$, then a new divergence appears in the PDF [11]. The shape of the exact PDF for the scaled exponent $\tilde{\lambda}_n = n(\lambda_n - \lambda_\infty)$ is illustrated in Fig. 1 for different values of n . Prasad and Ramaswamy proposed a smooth ansatz for the discontinuous expression (18), that in terms of the scaled variable reads

$$P(\tilde{\lambda}_n) = \frac{1}{\pi} \frac{\exp(-|\tilde{\lambda}_n|)}{\sqrt{1 - \exp(-2|\tilde{\lambda}_n|)}}, \quad (19)$$

for $\tilde{\lambda}_n \in (-\infty, n \ln 2]$. They based their conjecture on the analysis for small n . Here we will show that it is possible to advance further, developing expression (18) and evaluating it explicitly, therefore, finding analytically a smooth expression valid for large enough n .

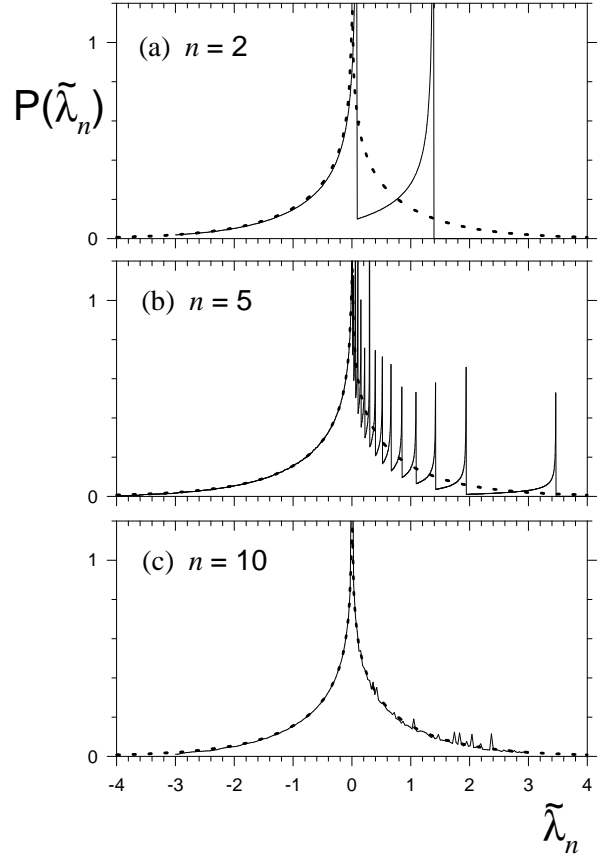


FIG. 1. Exact $P(\tilde{\lambda}_n)$ as a function of $\tilde{\lambda}_n \equiv n(\lambda_n - \lambda_\infty)$ (full lines), obtained numerically from Eq. (21), for different values of n indicated in the figure. As n increases divergences become narrower and cannot be appreciated unless one refines the mesh increasing the number of data exponentially with n . The dashed lines correspond to the smooth approximation given by (30).

Considering that $\sum_{j=0}^{n-1} \ln |f'(x_j)| = \ln |[f^n(x_0)]'|$ and making the transformation $x = \sin^2(\pi z/2)$, from Eq. (1), one gets the compact expression

$$\tilde{\lambda}_n = -\ln[\sin(\pi z)] + \ln |\sin(2^n \pi z)| \equiv F_n(z), \quad (20)$$

where the scaled exponent is expressed as a function of the state variable z (from now on the subindex 0 will be

omitted) evaluated at the instant at which the trajectory segment of time length n starts. The first logarithmic term is a smooth function in $[0, 1]$ that does not depend on n , while the second term is a periodic function with divergences at $z = j/2^n$, with $j \in \mathcal{Z}$ and $0 \leq j \leq 2^n$. Increasing n will increase the frequency and the comb of divergences will become more compact. The shape of $F_n(z)$ is illustrated in Fig. 2, for $n = 5$.

Since the invariant density of the attractor as a function of z is uniform, using (16), the PDF for $\tilde{\lambda}_n$ is given by

$$P(\tilde{\lambda}_n) = \int_0^1 dz \delta(\tilde{\lambda}_n - F_n(z)) = \sum_j \frac{1}{|F'_n(z_j^*)|}, \quad (21)$$

where z_j^* are such that $F_n(z_j^*) = \tilde{\lambda}_n$.

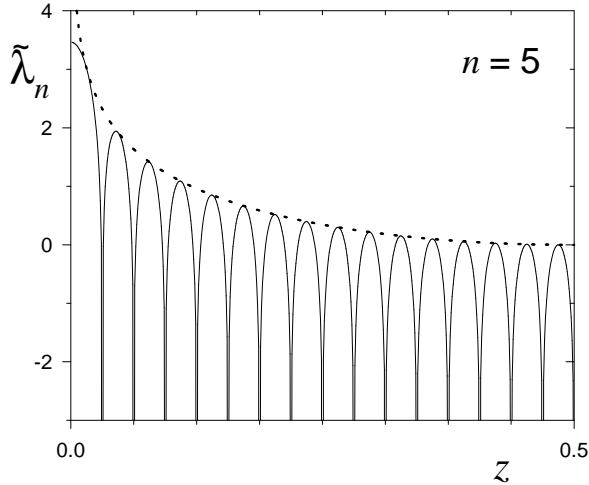


FIG. 2. Scaled Lyapunov exponent $\tilde{\lambda}_n \equiv F_n(z)$ as a function of z , the value of the state variable when the computation of the exponent is initiated (full lines). In this case $n = 5$. The dotted line corresponds to the smooth component $-\ln|\sin(\pi z)|$ that does not depend on n . Increasing n by one will double the number of periods. There is symmetry around $z = 1/2$, then only half of the full abscissae interval has been represented.

Let us separate the analysis into two cases according to the sign of $\tilde{\lambda}_n$.

(I) For $\tilde{\lambda}_n < 0$, the exact PDF is smooth. There is symmetry around $z = \frac{1}{2}$. In the interval $[0, \frac{1}{2}]$ there are $2^n - 1$ intersections at $z_{j\pm}^* = j/2^n \pm \delta_j$ such that $0 < \delta_j \ll j/2^n$. Taking into account that the main contribution to the derivative F'_n comes from the periodic component, then $|F'_n(z_{j\pm}^*)| \simeq \pi 2^n |\cos(2^n \delta_j \pi) / \sin(2^n \delta_j \pi)|$,

where, from (20), $|\sin(2^n \delta_j \pi)| \simeq \exp(\tilde{\lambda}_n) |\sin(j\pi/2^n)|$. Substitution of the derivatives in (21) leads to

$$P(\tilde{\lambda}_n) \simeq \frac{4e^{\tilde{\lambda}_n}}{\pi 2^n} \sum_{j=1}^{2^{n-1}} \frac{|\sin(j\pi/2^n)|}{\sqrt{1 - e^{2\tilde{\lambda}_n} \sin^2(j\pi/2^n)}}. \quad (22)$$

Replacing the summation by an integral by identifying $x = j/2^n$, we get

$$P(\tilde{\lambda}_n) \simeq \frac{4e^{\tilde{\lambda}_n}}{\pi} \int_0^{1/2} dx \frac{\sin(\pi x)}{\sqrt{1 - e^{2\tilde{\lambda}_n} \sin^2(\pi x)}}, \quad (23)$$

that gives

$$P(\tilde{\lambda}_n) \simeq \frac{2}{\pi^2} \ln[\coth(-\tilde{\lambda}_n/2)]. \quad (24)$$

The approximations here performed are expected to be good even for small n , namely $n \gtrsim 2$. In fact, a good agreement between the approximate and exact PDFs in this region is observed already for $n = 2$ (see Fig. 1).

(II) The domain $0 < \tilde{\lambda}_n \leq n \ln 2$ is more tricky. At each local maximum of $F_n(z)$, a divergence in the PDF appears, as it follows from (21). Then, in this region, the PDF possesses 2^{n-1} spikes. Let us consider the interspike intervals $(\tilde{\lambda}^-, \tilde{\lambda}^+]$ determined by two successive values of z at which $F'_n = 0$. In each interspike interval the PDF monotonously increases, because $|F'_n|$ decreases with increasing $\tilde{\lambda}_n$ (see Fig. 2), and diverges at the upper limit of the interval $\tilde{\lambda}^+$, where $F'_n = 0$. These behaviors can be observed in Fig. 1, for $n = 2$ and 5. As n increases, although the cusps increase exponentially in number, they get thinner, in such a way that they will become invisible in numerical histograms due to the finiteness of bin size. Then, if n is large enough, histograms would look smooth although the exact PDF is not, unless one could make the bin size arbitrarily small. In such case, the higher the resolution, the larger the height of the spikes. However, in practice, there are constraints to reach an arbitrarily fine resolution due to finiteness of numerical data sets. This fact turns it useful to find a smooth expression to describe the histograms actually observed for not too small n . In order to do so, we have to calculate the probability $\int_{bin} d\tilde{\lambda} P(\tilde{\lambda})$ associated to a finite bin of the order of (or larger than) the interspike distance $\Delta\tilde{\lambda} = \tilde{\lambda}^+ - \tilde{\lambda}^-$.

For each diffeomorphic branch of F_n one has $F'_n(z) = F'_n(F_n^{-1}(\tilde{\lambda}_n)) = 1 / [\frac{dF_n^{-1}(\tilde{\lambda}_n)}{d\tilde{\lambda}_n}]$, then, from Eq. (21), the probability that $\tilde{\lambda}_n$ belongs to the interval $(\tilde{\lambda}^-, \tilde{\lambda}^+]$ is given by

$$\int_{\Delta\tilde{\lambda}} d\tilde{\lambda} P(\tilde{\lambda}) = 2 \sum_{i=1}^m \left| F_i^{-1}(\tilde{\lambda}^+) - F_i^{-1}(\tilde{\lambda}^-) \right| = 2 \sum_{i=1}^m \Delta z_i, \quad (25)$$

where Δz_i are the segments displayed in Fig. 3, corresponding to the inverse images of $\Delta\tilde{\lambda}$. The summation runs up to a value m that depends on the particular interval chosen and that is given by the smooth component of F_n .

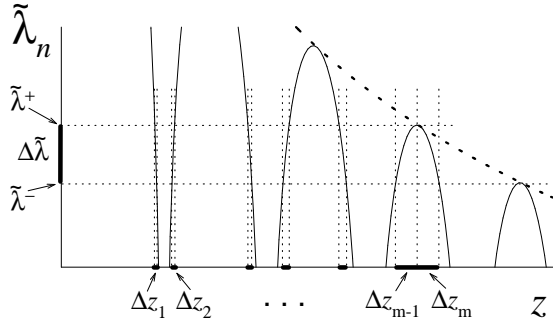


FIG. 3. Schematic representation of the scaled Lyapunov exponent $\tilde{\lambda}_n$ as a function of z . The segments on the horizontal axis represent the contributions to the probability associated to the interspike interval $\Delta\tilde{\lambda} \equiv \tilde{\lambda}^+ - \tilde{\lambda}^-$.

This procedure will give rise to a discrete PDF where the integrated probabilities (25) can be attributed, for instance, to the midpoints $\tilde{\lambda}^*$ of each interval $\Delta\tilde{\lambda}$, such that

$$P(\tilde{\lambda}^*) \simeq \frac{\int_{\Delta\tilde{\lambda}} d\tilde{\lambda} P(\tilde{\lambda})}{\Delta\tilde{\lambda}} = 2 \sum_{i=1}^m \frac{\Delta z_i}{\Delta\tilde{\lambda}}. \quad (26)$$

Now, $\frac{\Delta\tilde{\lambda}}{\Delta z_i} \simeq |F'_n(z_i^*)|$, where the derivative is evaluated at the midpoint z_i^* of the interval Δz_i . As the derivative F'_n is dominated by the periodic component in Eq. (20), one can perform an analysis analogous to that for case (I), obtaining

$$P(\tilde{\lambda}^*) \simeq \frac{4e^{\tilde{\lambda}^*}}{\pi 2^n} \sum_{j=1}^{j_{max}} \frac{|\sin(j\pi/2^n)|}{\sqrt{1 - e^{2\tilde{\lambda}^*} \sin^2(j\pi/2^n)}}, \quad (27)$$

where $j_{max} \simeq 2^n \arcsin[\exp(-\tilde{\lambda}^*)]/\pi$, for $\tilde{\lambda}^* \in (\tilde{\lambda}^-, \tilde{\lambda}^+)$. Replacing the summation by an integral as in case (I), one obtains

$$P(\tilde{\lambda}^*) \simeq \frac{4e^{\tilde{\lambda}^*}}{\pi} \int_0^{\theta(\tilde{\lambda}^*)} dx \frac{\sin(\pi x)}{\sqrt{1 - e^{2\tilde{\lambda}^*} \sin^2(\pi x)}}, \quad (28)$$

where $\theta(\tilde{\lambda}^*) = \arcsin[\exp(-\tilde{\lambda}^*)]/\pi$. After integration, one arrives at

$$P(\tilde{\lambda}^*) \simeq \frac{2}{\pi^2} \ln[\coth(\tilde{\lambda}^*/2)]. \quad (29)$$

Let us recall that, in contrast to case (I), here we have a discrete PDF defined for the middle points of the interspike intervals. However, since the interspike distance $\Delta\tilde{\lambda}$ goes to zero for increasing n and not too large $\tilde{\lambda}_n$, one can smooth the staircase function (29) by extending it to every point of the interval $(0, n \ln 2]$. In that case, one gets the symmetric counterpart of expression (24).

Expressions (24) and (29) can be gathered into the single expression

$$P(\tilde{\lambda}_n) \simeq \frac{2}{\pi^2} \ln(\coth|\tilde{\lambda}_n/2|). \quad (30)$$

This result explains the apparent symmetry of numerical PDFs for large n despite the fact that left and righthand wings of the distribution have very different genealogies. For large $|\tilde{\lambda}_n|$, the PDF decays exponentially, yielding straight lines in the semi-log representation displayed in Fig. 4. Notice that the approximate distribution (30) for the scaled variable $\tilde{\lambda}_n$ does not depend on n . In particular, it is expected to be exact in the limit $n \rightarrow \infty$. That is, (30) is a good representation of the delta function to which the finite-time distribution asymptotically collapses. Remarkably enough, the approximations that led to (30) did not spoil the normalization condition, i.e., $\int_{-\infty}^{\infty} d\tilde{\lambda} P(\tilde{\lambda}) = 1$ holds.

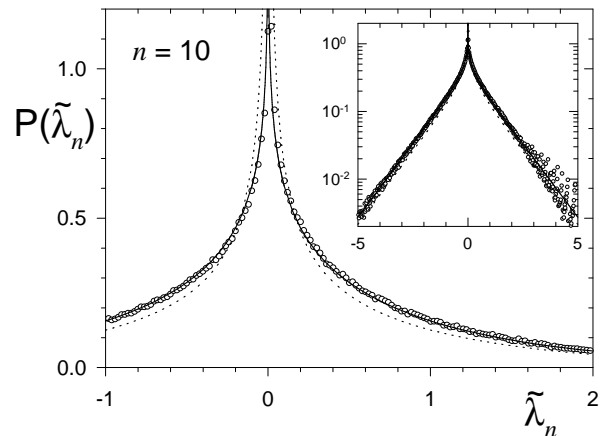


FIG. 4. $P(\tilde{\lambda}_n)$ as a function of $\tilde{\lambda}_n$ for $n = 10$. Small symbols correspond to the histogram accumulated over 10^6 histories obtained through numerical iterations of the map, after a transient of 10^3 time steps. The bin size is 0.02. Expressions (30) (full line) and (19) (dotted line) are plotted for comparison. Inset: the same data in semi-log representation allow to appreciate the tails. The spikes in the righthand tail of the histogram are visible for large $\tilde{\lambda}_n$ where they become more sparse and are amplified by the logarithmic scale.

In Fig. 4 the approximation (30) is compared to an histogram obtained from numerical iterations of the mapping. The analytical prediction is in very good accord with numerical results and it describes the numerical data more accurately than the ansatz (19). Notably, the variance of the scaled exponent $\tilde{\lambda}_n = n(\lambda_n - \lambda_\infty)$ calculated with our PDF is $\tilde{\sigma}^2 = \pi^2/6$. Then for exponent λ_n one obtains $\sigma^2(n) = \pi^2/(6n^2)$ which coincides with the exact result (15), if neglecting the term of order $1/2^n$ (the order of the performed approximations). In contrast, the ansatz of ref. [11] gives $\sigma^2(n) = (\pi^2/12 + [\ln 2]^2)/n^2 \simeq 0.79 \pi^2/(6n^2)$, i.e., more than 20% smaller than the true value.

As an aside comment, notice that in the exact distribution the ordinate at the origin increases with n but is finite for finite n . However, expression (30) diverges at $\tilde{\lambda}_n = 0$ (as also (19) does). In the exact PDF, divergences appear for positive abscissae only and accumulate close to the origin as n increases. Therefore, strictly speaking, a divergence at the origin is expected in the limit $n \rightarrow \infty$ only.

SUMMARY AND FINAL REMARKS

We have derived analytical results for the statistics of finite-size exponents on the logistic map at the Ulam point. In particular, we have found the exact analytical expression (15) for the variance of local exponents, putting into evidence the origin of its anomalous time decay. Moreover, we have found the smooth analytical PDF (30), expected to be the exact one in the limit $n \rightarrow \infty$. Therefore, we have extended the work initiated by Prasad and Ramaswamy [11], providing a complete and consistent picture of the statistical properties of finite time Lyapunov exponents at an outer crisis.

As the special shape of the distribution of finite-time exponents at the Ulam point is also seen in other systems presenting fully developed chaos [11], our results are expected to be useful for more general systems falling into the same class. In addition, these analytical results could give insights on features occurring in the synchronization transition of lattices of coupled chaotic maps [8], such as hiperbolicity breakdown through unstable dimension variability [9], since the distribution of finite-time Lyapunov

exponents in the synchronized states of such networks is related to the distribution of local exponents in the uncoupled map [10].

C. A. is grateful to Sandro E. de S. Pinto and Ricardo L. Viana for very stimulating discussions, and to Raúl O. Vallejos for his usual insightful remarks. C. A. acknowledges brazilian agencies FAPERJ and PRONEX for financial support.

-
- [1] V.I. Oseledec, *Trans. Mosc. Math. Soc.* **19**, 197 (1968).
 - [2] J.-P. Eckmann and D. Ruelle, *Rev. Mod. Phys.* **57**, 617 (1985).
 - [3] E. Ott., *Chaos in Dynamical Systems* (Cambridge University Press, 1993).
 - [4] K. Nam, E. Ott, T. M. Antonsen, Jr., and P. N. Guzdar, *Phys. Rev. Lett.* **84**, 5134 (2000); G. Boffetta, A. Celani, and S. Musacchio, *Phys. Rev. Lett.* **91**, 034501 (2003).
 - [5] F.M. Cucchietti, C.H. Lewenkopf, E.R. Mucciolo, H.M. Pastawski and R.O. Vallejos, *Phys. Rev. E* **65**, 046209 (2002).
 - [6] C. Beck and F. Schlögl, *Thermodynamics of chaotic systems* (Cambridge University Press, 1993).
 - [7] S. Dawson, C. Grebogi, T. Sauer and J.A. Yorke, *Phys. Rev. Lett.* **73**, 1927 (1994).
 - [8] A.M. Batista and R.L. Viana, *Phys. Lett. A* **286**, 134 (2001); A.M. Batista, S.E.D. Pinto, R.L. Viana and S.R. Lopes, *Phys. Rev. E* **65**, 056209 (2002).
 - [9] R.L. Viana, C. Grebogi, S.E. de S. Pinto, S.R. Lopes, A.M. Batista and J. Kurths (unpublished).
 - [10] C. Anteneodo, S.E. de S. Pinto, A.M. Batista and R.L. Viana, LANL preprint nlin.CD/0308014.
 - [11] A. Prasad and R. Ramaswamy, *Phys. Rev. E* **60**, 2761 (1999).
 - [12] H. Fujisaka, *Prog. Theor. Phys.* **70**, 1264 (1983).
 - [13] A.J. Lichtenberg and M.A. Leiberman, *Regular and Chaotic Dynamics* (John Wiley & Sons, 1992).
 - [14] T. Nagashima and H. Haken, *Phys. Lett. A* **96**, 385 (1983).
 - [15] S. Grossmann and S. Thomae, *Z. Naturforsch.* **32a**, 1353 (1977).
 - [16] H.-P. Herzog and W. Ebeling, *Phys. Lett. A* **111**, 1 (1985); errata: **111**, 457 (1985).